

Electronic Supplementary Information

Composition-dependent surface chemistry of colloidal $\text{Ba}_x\text{Sr}_{1-x}\text{TiO}_3$ perovskite nanocrystals

Tigran Margossian,^a Sean P. Culver,^b Kim Larmier,^a Feng Zhu,^c Richard L. Brutchey^{b,*} and Christophe Copéret^{a,*}

^a ETH Zürich, Department of Chemistry and Applied Biosciences, Vladimir-Prelog-Weg 2, CH-8093 Zürich, Switzerland

^b Department of Chemistry, University of Southern California, Los Angeles, CA 90089, USA

^c Department of Chemistry, Iowa State University, Ames, IA 50011, USA

Email: ccoperet@inorg.chem.ethz.ch, brutchey@usc.edu

Experimental

General procedures. All manipulations were conducted under nitrogen atmosphere using standard Schlenk techniques. All reagents were used as received. Solutions of the double metal alkoxides $\text{BaTi}(\text{OR})_6$ and $\text{SrTi}(\text{OR})_6$ ($\text{R} = \text{CH}_2\text{CHCH}_3(\text{OCH}_3)$) in *n*-butanol/2-methoxypropanol (1:3 v/v, bp 117 °C) from Gelest, Inc. were employed as precursors for the synthesis of colloidal $\text{Ba}_{1-x}\text{Sr}_x\text{TiO}_3$ nanocrystals. The molarities of the bimetallic alkoxide solutions were 0.50 and 0.70 M for $\text{BaTi}(\text{OR})_6$ and $\text{SrTi}(\text{OR})_6$, respectively.

Apparatus. The apparatus employed for the synthesis of colloidal $\text{Ba}_{1-x}\text{Sr}_x\text{TiO}_3$ nanocrystals via vapor diffusion sol-gel (VD SG) consists of a 100-mL three-neck reaction flask and a glass bubbler containing a 0.75 M HCl solution. The bubbler is connected to the nitrogen manifold via a needle-valve rotameter. Nitrogen gas is bubbled through the 0.75 M HCl solution for 30 min, while one or more bimetallic alkoxide precursors are transferred to the reaction flask via syringe. Then, the bubbler is connected to the reaction flask in order to allow $\text{N}_2/\text{HCl}/\text{H}_2\text{O}$ vapor to continuously flow over the precursor solution at room temperature and atmospheric pressure.

Synthesis of $\text{Ba}_{1-x}\text{Sr}_x\text{TiO}_3$ nanocrystals. One or more bimetallic alkoxide precursors are added to the reaction flask to obtain the desired stoichiometry and a total volume of 2.00 mL (approximate exposed liquid area: 3 cm²). For example, 2.0 mL (1.0 mmol) of $\text{BaTi}(\text{OR})_6$ were employed in the synthesis of BaTiO_3 nanocrystals. Mixtures of two bimetallic alkoxides were magnetically stirred for 20 min to ensure intimate mixing; then, the stir bar was removed. The one-step synthesis consisted of flowing $\text{N}_2/\text{HCl}/\text{H}_2\text{O}$ vapor over the precursor solution for 36 h. The solution turned into a fully rigid gel a few hours (~7 h) after starting the vapor flow, followed by cracks and the expulsion of a clear supernatant. After 36 h, the vapor flow is stopped, the reaction flask opened, and pieces of the gel collected. These were washed with 5 mL of absolute ethanol, sonicated for 10 min, and centrifuged at 6000 rpm for 25 min. This washing step was repeated three times. The resulting nanocrystals were dried under vacuum at room temperature for 4 h, yielding a fine, off-white powder. Inside an inert atmosphere glovebox, the resulting powder was transferred to a flow tubular quartz reactor. The sample was calcined at 600 °C under a synthetic air stream (0.2 O₂/0.8 N₂) with a temperature ramp of 1 °C min⁻¹. The powder was then degassed under high vacuum (10⁻⁵ mbar) for 30 min and transferred to the glovebox.

Material characterization. *Elemental analysis:* The chemical composition of the $\text{Ba}_{1-x}\text{Sr}_x\text{TiO}_3$ nanocrystals was determined using inductively coupled plasma atomic emission spectroscopy (ICP-AES) (Galbraith Labs, Knoxville, TN). *Thermal analysis:* Thermal analysis measurements were made on a Netzsch DSC/TGA - MS/IR STA449 F1 using sample sizes of ~ 20 mg. Argon was used as a protective and flow gas. Mass flow controllers were set to 40 mL min^{-1} for the protective gas and 10 mL min^{-1} for the purge gas. The thermal range examined was $50\text{-}500 \text{ }^\circ\text{C}$ with a heating rate of $10 \text{ }^\circ\text{C min}^{-1}$. *N_2 adsorption at 77 K:* Nitrogen adsorption–desorption at 77 K was measured on a Bel-Mini from BelJAPAN. Before the measurement, the samples were transferred from the glovebox to the Bel-Mini using an airtight cell. Total surface area was calculated using the BET method and the pore volume using the BJH adsorption method. *Transmission electron microscopy (TEM):* TEM images were collected with a Philips CM12 transmission electron microscope. All samples were dispersed in absolute ethanol using ultrasound prior to the grid preparation. The particle size distributions were obtained from a minimum of 150 nanocrystals. *Powder X-ray diffraction (XRD):* XRD patterns were collected with STOE STADI P powder diffractometer, operating in transmission mode. A germanium monochromator, $\text{Cu K}\alpha_1$ irradiation, and Dectris Mythen silicon strip detector were used. *FT-IR measurement:* Transmission IR spectra were recorded on a Bruker Alpha-T spectrometer inside the glovebox. Samples were pressed into a thin pellet using a 7-mm die set. The spectra were recorded with 24 scans at a resolution of 4 cm^{-1} . *ssNMR measurement:* All solid-state ^{13}C NMR spectra were recorded on a Bruker AVANCE III 700 MHz spectrometer. Chemical shifts are reported in ppm downfield from liquid SiMe_4 (0 ppm). A 4-mm rotor containing the samples was spun at a rate of 10 kHz and 8192 scans was recorded using HPDEC sequence. Low spinning experiment is recorded in 4-mm rotor at a spinning rate of 4 kHz (32768 scans, HPDEC sequence).

Surface characterization (ssNMR/FT-IR) of the nanocrystals dosed with CO_2 . Inside the inert atmosphere glovebox, transmission FT-IR spectra of freshly calcined $\text{Ba}_{1-x}\text{Sr}_x\text{TiO}_3$ was measured and 150 mg of this material is loaded inside a Schlenk cell ($V \approx 20 \text{ mL}$). The sample was degassed under high vacuum (10^{-5} mbar) for 30 min at $25 \text{ }^\circ\text{C}$. At $25 \text{ }^\circ\text{C}$, an excess of carbon dioxide ($\approx 4 \text{ CO}_2 \text{ nm}^{-2}$) was introduced inside the Schlenk cell, and the CO_2 was left in contact with the sample for 30 min. The sample was then degassed under high vacuum (10^{-5} mbar) for 30 min at $25 \text{ }^\circ\text{C}$. A transmission FT-IR of spectrum of the CO_2 - $\text{Ba}_{1-x}\text{Sr}_x\text{TiO}_3$ measurement was carried out under inert conditions. Samples for ssNMR characterization were similarly prepared, except with $^{13}\text{CO}_2$.

CO_2 temperature programmed desorption (TPD). These experiments were carried out using a BELCAT-B from BEL JAPAN equipped with a CATCryo system allowing a linear temperature control from 223-1213 K. CO_2 -TPD was performed on 100 mg of calcined $\text{Ba}_{1-x}\text{Sr}_x\text{TiO}_3$ that was pre-treated at $300 \text{ }^\circ\text{C}$ in He (30 mL min^{-1}) for 2 h using a ramp of $5 \text{ }^\circ\text{C min}^{-1}$. The sample was then cooled down to $25 \text{ }^\circ\text{C}$ under He for 45 min and then to $-50 \text{ }^\circ\text{C}$ under CO_2 for 1 h. The TPD measurement was performed from $-50 \text{ }^\circ\text{C}$ to $900 \text{ }^\circ\text{C}$ under He using a ramp of 10 K min^{-1} . The CO_2 uptake was followed using a calibrated TCD detector and a mass spectrometer set with $m/z = 15, 18, 28$ and 44 .

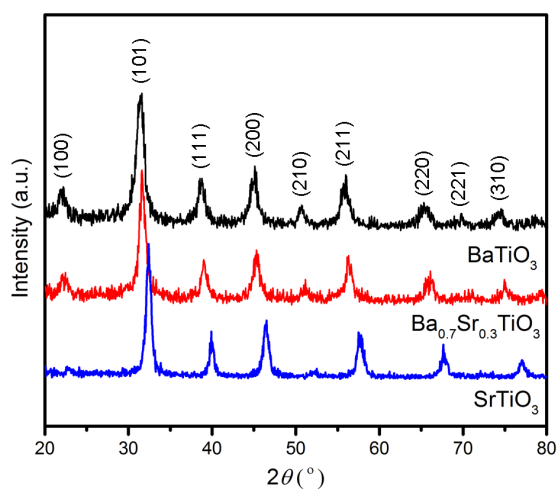


Fig. S1 Powder XRD of the as-prepared nanocrystals. Key: black (BaTiO_3), red ($\text{Ba}_{0.7}\text{Sr}_{0.3}\text{TiO}_3$), blue (SrTiO_3).

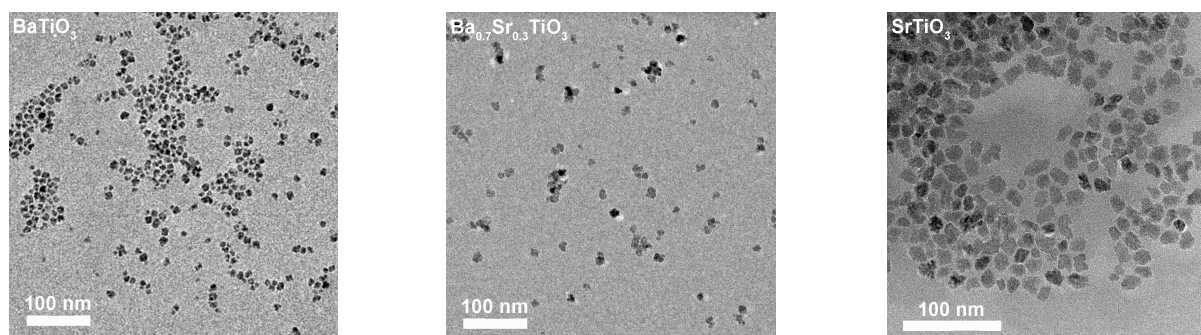


Fig. S2 TEM images of the as-prepared nanocrystals. Key: left (BaTiO_3), middle ($\text{Ba}_{0.7}\text{Sr}_{0.3}\text{TiO}_3$), right (SrTiO_3).

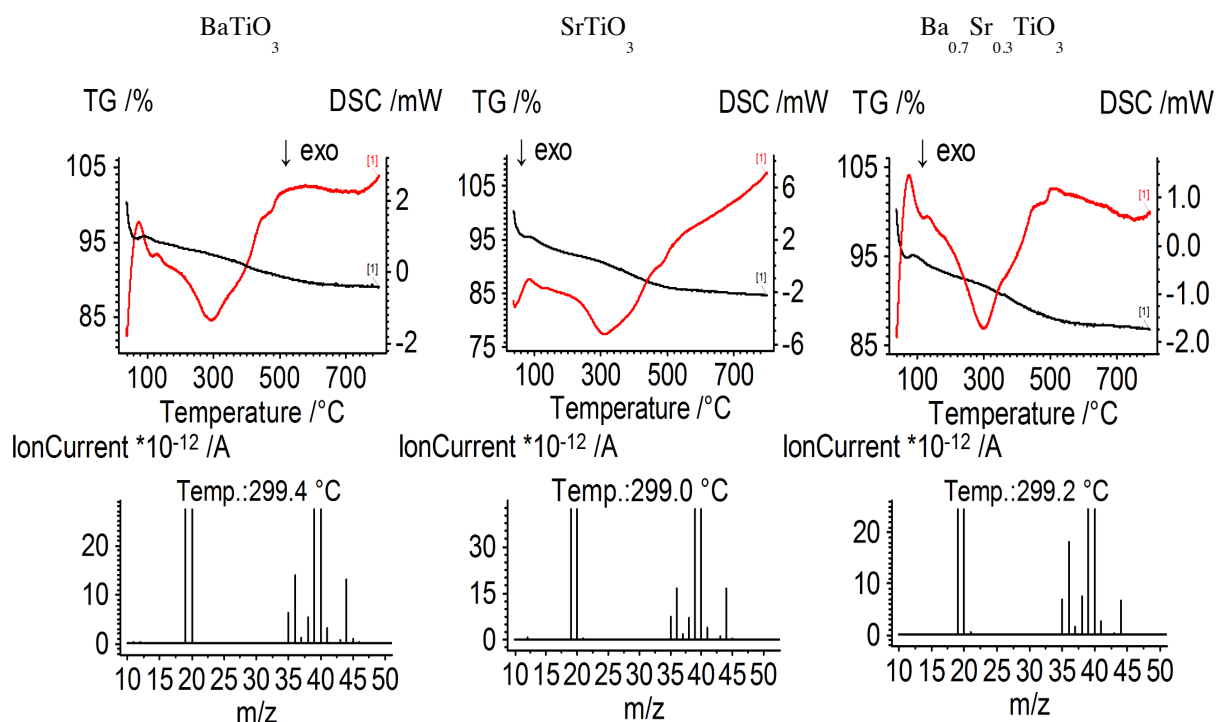


Fig. S3 TGA/DSC-MS of the as-prepared nanocrystals run at a heating rate of 10 °C min⁻¹ under flowing Ar. Key: left (BaTiO₃), middle (Ba_{0.7}Sr_{0.3}TiO₃), right (SrTiO₃).

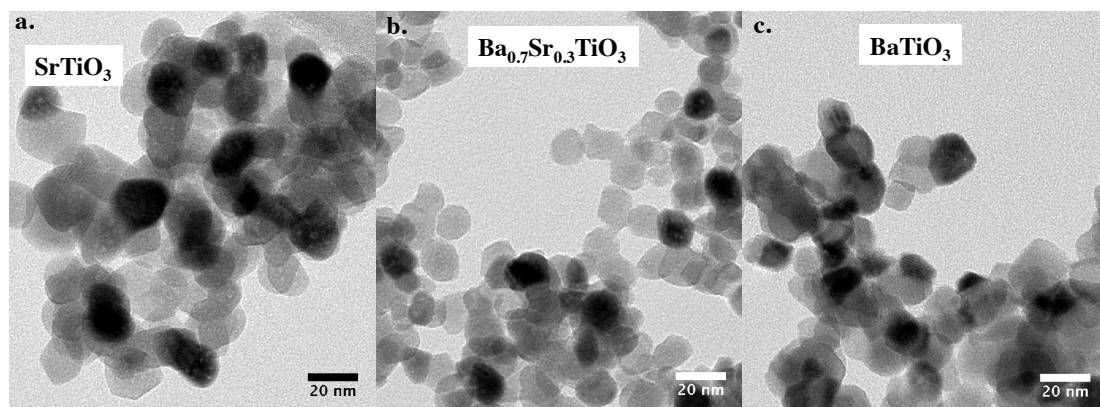


Fig. S4 TEM images of the calcined nanocrystals. Key: (a) SrTiO₃, (b) Ba_{0.7}Sr_{0.3}TiO₃, (c) BaTiO₃.

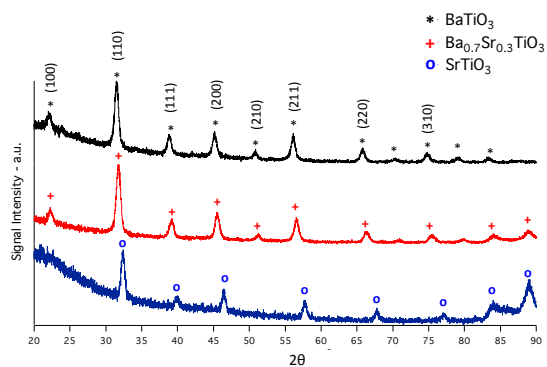


Fig. S5 Powder XRD of the calcined nanocrystals. Key: black (BaTiO₃), red (Ba_{0.7}Sr_{0.3}TiO₃), blue (SrTiO₃).

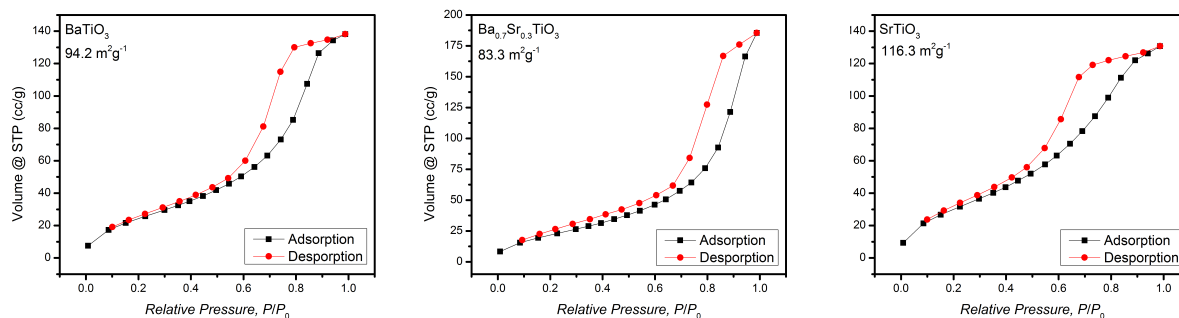


Fig. S6 Nitrogen adsorption/desorption isotherms of the as-prepared nanocrystals. Key: left (BaTiO_3), middle ($\text{Ba}_{0.7}\text{Sr}_{0.3}\text{TiO}_3$), right (SrTiO_3).

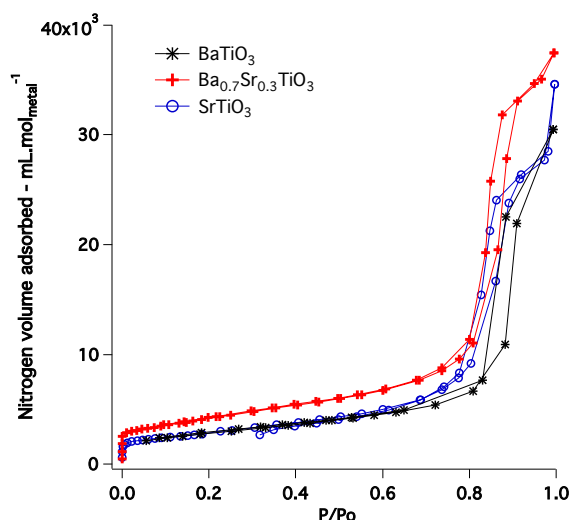


Fig. S7 Nitrogen adsorption/desorption isotherms of the calcined nanocrystals. Key: black ($S_{\text{BET}} = 41 \text{ m}^2.\text{g}^{-1}$ BaTiO_3), red ($S_{\text{BET}} = 75 \text{ m}^2.\text{g}^{-1}$ $\text{Ba}_{0.7}\text{Sr}_{0.3}\text{TiO}_3$), blue ($S_{\text{BET}} = 56 \text{ m}^2.\text{g}^{-1}$ SrTiO_3).

The specific surface area is directly connected to the material weight. As the molecular weight is varying dramatically between the different samples ($\text{Ba}_{1-x}\text{Sr}_x\text{TiO}_3$ with $0 \leq x \leq 1$), we decided to normalize their value per mole of (ATiO_3) units instead of per gram of sample using the Equation SI 1.

$$S_{\text{BET},n}(\text{m}^2.\text{mol}^{-1}) = S_{\text{BET},m}(\text{m}^2.\text{g}^{-1}) \times M_{\text{Ba}_x\text{Sr}_{1-x}\text{TiO}_3}(\text{g}.\text{mol}^{-1}) \quad \text{Equation. SI1}$$

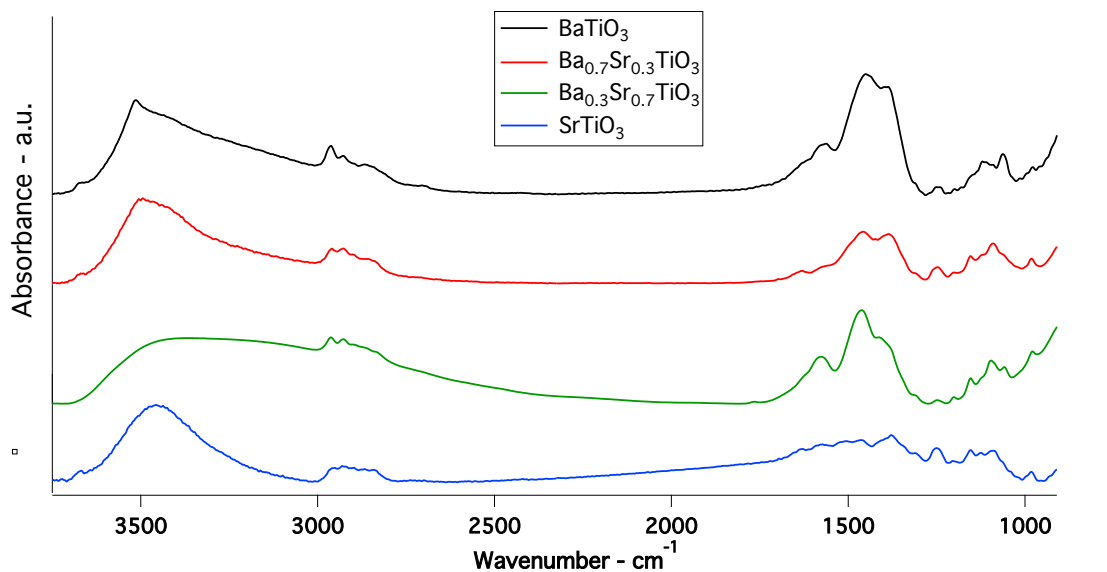


Fig. S8 FT-IR spectra of the as-prepared nanocrystals with material diluted in KBr (1/10 wt/wt) Key: black (BaTiO_3), red ($\text{Ba}_{0.7}\text{Sr}_{0.3}\text{TiO}_3$), green ($\text{Ba}_{0.3}\text{Sr}_{0.7}\text{TiO}_3$), blue (SrTiO_3).

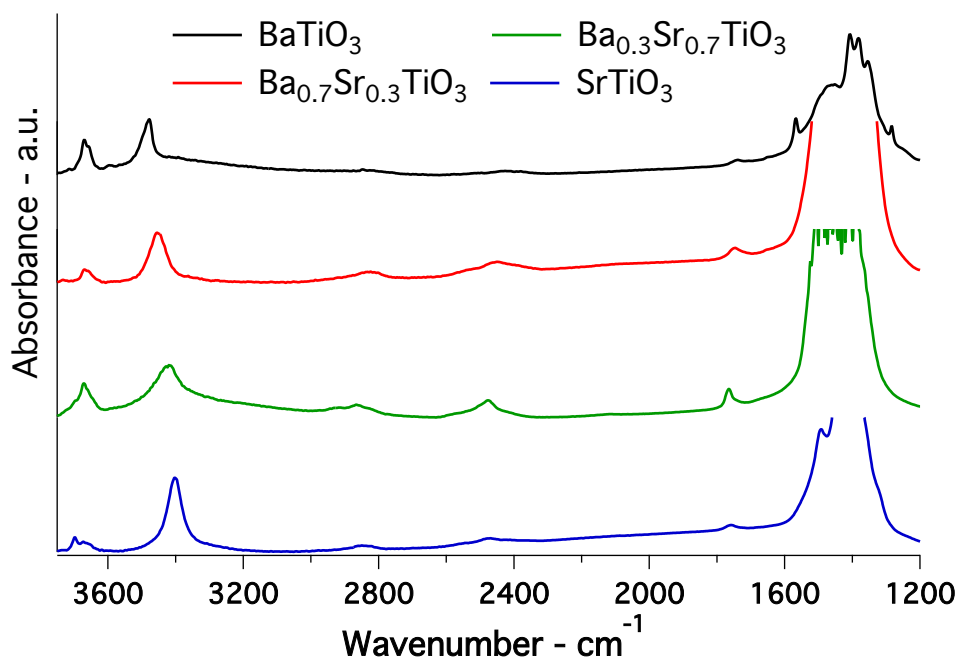


Fig. S9 FT-IR spectra of the nanocrystals dehydrated and calcined to 600 °C Key: black (BaTiO_3), red ($\text{Ba}_{0.7}\text{Sr}_{0.3}\text{TiO}_3$), green ($\text{Ba}_{0.3}\text{Sr}_{0.7}\text{TiO}_3$), blue (SrTiO_3).

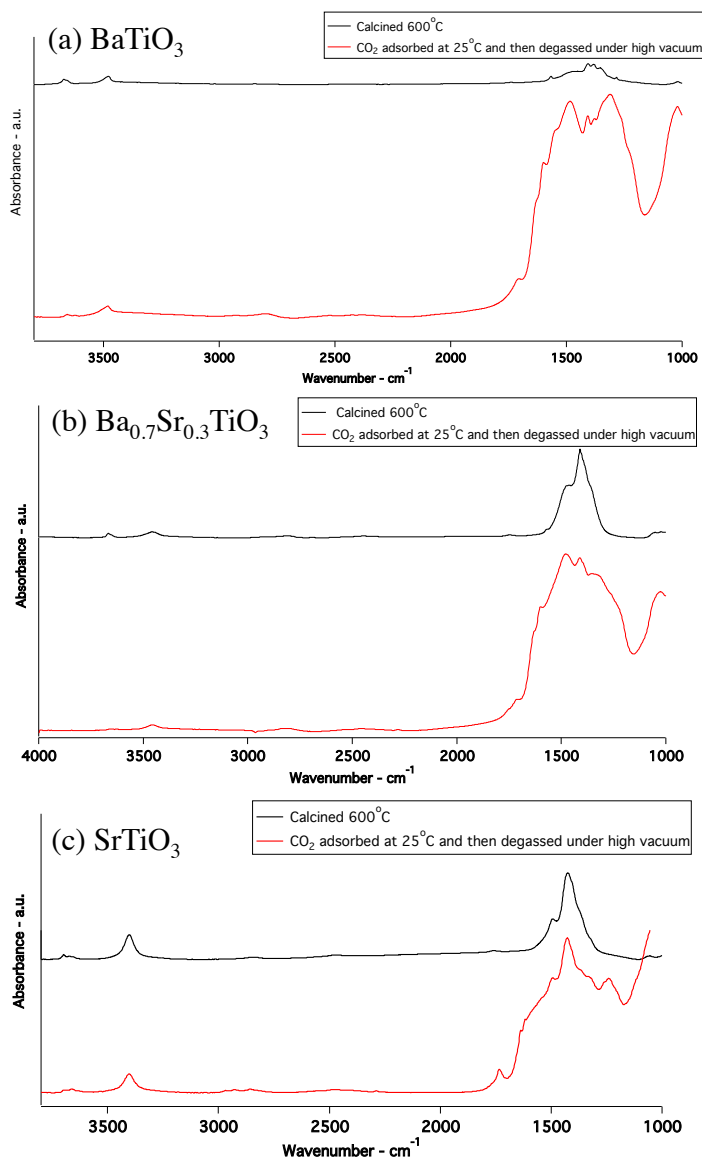


Fig. S10 FT-IR spectra of CO₂ adsorbed on the calcined nanocrystals. (a) BaTiO₃, (b) Ba_{0.7}Sr_{0.3}TiO₃, and (c) SrTiO₃ nanocrystals. Key: black (calcined nanocrystals prior to exposure to CO₂), red (after CO₂ adsorption at 25 °C and degassing under high vacuum).

Table S1. FT-IR vibrational frequencies of carbonate species in Fig. S10.

	Peak 1 cm ⁻¹	Peak 2 cm ⁻¹	Peak 3 cm ⁻¹	Peak 4 cm ⁻¹	Peak 5 cm ⁻¹	Peak 6 cm ⁻¹	Peak 7 cm ⁻¹	Peak 8 cm ⁻¹	Peak 9 cm ⁻¹	Peak 10 cm ⁻¹	Peak 11 cm ⁻¹	Peak 12 cm ⁻¹
BaTiO ₃	1706	1634	1598	1553	1483	1408	1378	1311	-	-	-	1020
Ba _{0.7} Sr _{0.3} TiO ₃	1711	-	1598	-	1478	1411	1358	-	-	-	1054	1025
SrTiO ₃	1735	1637	1618	1541	1495	1429	1365	1328	1259	1166	1055	-

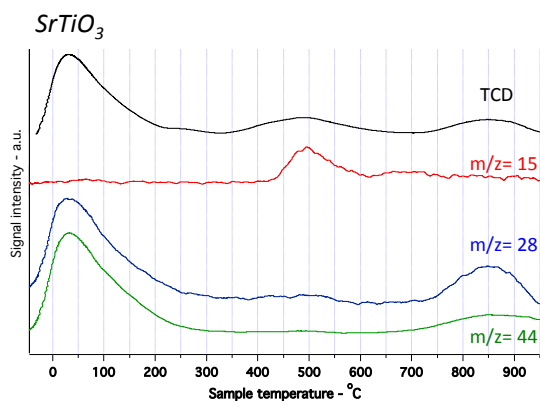


Fig. S11 CO₂-TPD profile for calcined SrTiO₃ nanocrystals. 150 mg of sample was used for measurement. Key: black (TCD), red ($m/z = 15$), blue ($m/z = 28$), green ($m/z = 44$).

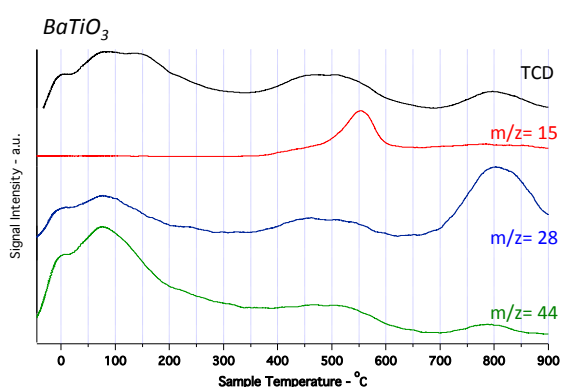


Fig. S12 CO₂-TPD profile for calcined BaTiO₃ nanocrystals. 150 mg of sample was used for measurement. Key: black (TCD), red ($m/z = 15$), blue ($m/z = 28$), green ($m/z = 44$).

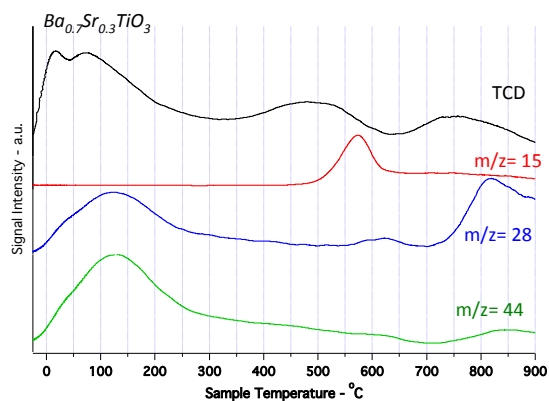


Fig. S13 CO₂-TPD profile for calcined Ba_{0.7}Sr_{0.3}TiO₃ nanocrystals. 150 mg of sample was used for measurement. Key: black (TCD), red ($m/z = 15$), blue ($m/z = 28$), green ($m/z = 44$).

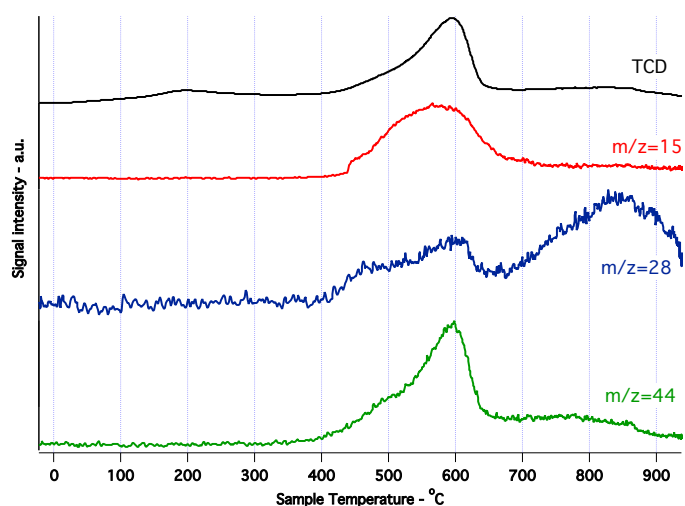


Fig. S14 Blank TPD profile for calcined BaTiO₃ nanocrystals. 150 mg of sample was used for measurement. Key: black (TCD), red ($m/z = 15$), blue ($m/z = 28$), green ($m/z = 44$).

Table S2. Parameters extracted from TCD signal decomposition of the CO₂-TPD experiment.

	Peak 1		Peak 2		Peak 3		Peak 4		Peak 5	
	°C ^a	% ^b								
BaTiO₃	-7	3	67	16	175	32	477	38	800	11
Ba_{0.7}Sr_{0.3}TiO₃	7	6	71	20	182	24	480	32	787	18
SrTiO₃	19	13	68	27	174	8	494	27	848	25

a: Desorption temperature estimated from peak fitting

b: Area fraction for each peak estimated from fitting

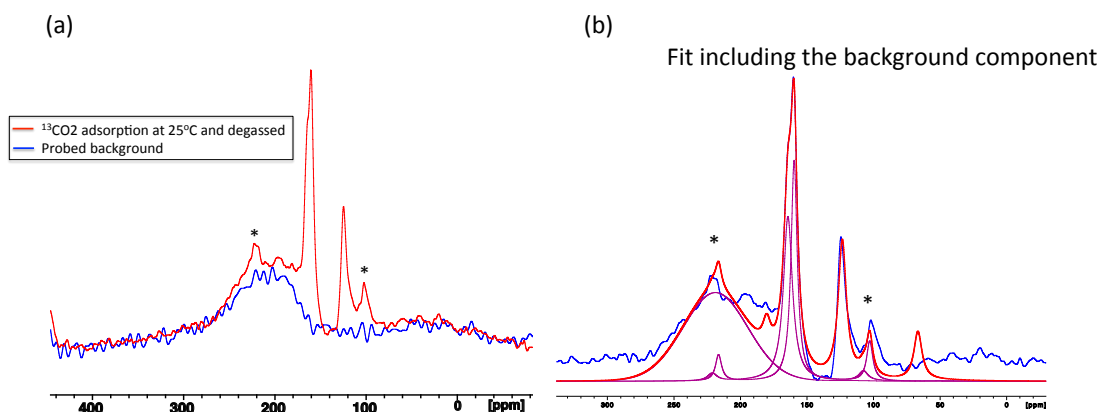


Fig. S15 $^{13}\text{CO}_2$ adsorption tracked by HPDEC ^{13}C ssNMR spectroscopy for SrTiO_3 , where * are indicating the spinning side band. (a) Spectrum (red) + probed background (blue); (b) Spectrum (blue) + fit including the background component (red).

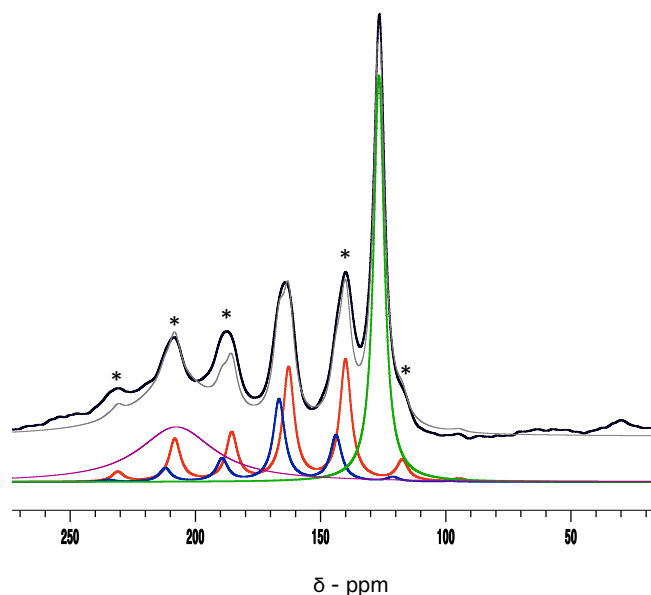


Fig. S16 $^{13}\text{CO}_2$ adsorption tracked by HPDEC ^{13}C ssNMR spectroscopy at 4 kHz for SrTiO_3 , where * are indicating the spinning side bands. Spectrum (black) + fit including the background component (grey).

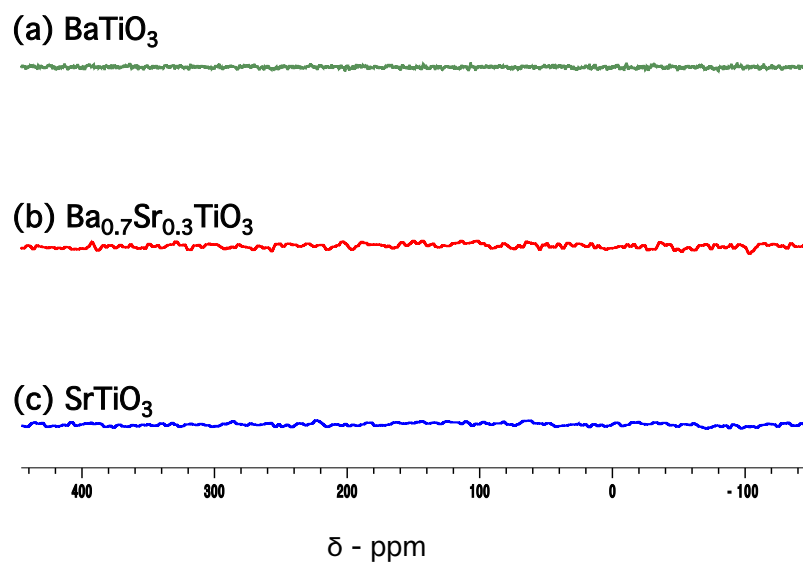


Fig. S17 ^{13}C adsorption tracked by HPDEC ^{13}C ssNMR spectroscopy for (a) BaTiO_3 , green (b) $\text{Ba}_{0.7}\text{Sr}_{0.3}\text{TiO}_3$, red (c) SrTiO_3 , blue desorption at 50°C .

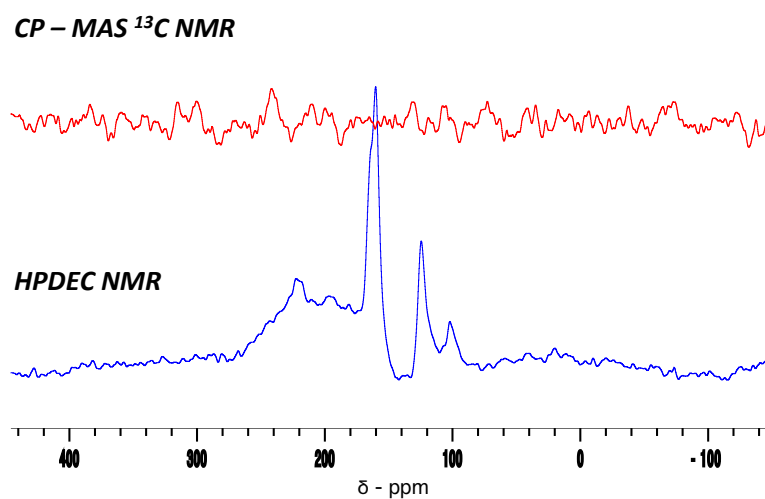


Fig. S18 ^{13}C adsorption on SrTiO_3 tracked by HPDEC ^{13}C ssNMR spectroscopy (blue, bottom) and tracked by CP-MAS ^{13}C ssNMR spectroscopy (red, top)

Table S3. Parameter results found for CSA fitting of the different spectra

	Peak 1 ^a				Peak 2				Peak 3			
	δ_{iso} - ppm	Ω - ppm	κ	Proportion - %	δ_{iso} - ppm	Ω - ppm	κ	Proportion - %	δ_{iso} - ppm	Ω - ppm	κ	Proportion - %
BaTiO ₃	-	-	-	-	162.1	131.8	-0.34	84	166.1	96.9	-0.95	16
Ba _{0.7} Sr _{0.3} TiO ₃	126.4	-	-	-	161.9	130.5	0.35	72	165.2	85.6	-1	11
Ba _{0.7} Sr _{0.3} TiO ₃ degassed 33 °C	-	-	-	-	-	-	-	-	165.4	77.6	-1	100
SrTiO ₃	123.5	-	-	32	160.0	125.1	-0.89	35	164.4	76.5	-0.9	33
SrTiO ₃ ^b	126.5	0.2	-0.9	38	164	103.0	-0.77	39	166.6	77.1	-0.95	23

a: No CSA parameter extracted because no spinning-side are observed
b: Low-spinning experiment (4 kHz), ns = 32 768 scans, 8 CO₂ nm⁻²

DFT Methods. Periodic DFT+D3 calculations have been carried out using VASP.^{1,2} The GGA-PBE functional was used,³ and the core electrons are computed using the PAW pseudo-potential approach.⁴ Dispersion forces are simulated according to the approach by Grimme (DFT+D3).⁵ The criterion convergence chosen for the SCF cycle was 10⁻⁵ eV, and optimizations were considered converged once the forces on all atoms were lower than 0.1 eV.Å⁻¹.

Bulk structures for BaTiO₃ and SrTiO₃ have been constructed with lattice parameters of 4.0140 and 3.9074 Å, respectively, as determined from the XRD diffraction patterns. Then, 10 Å-thick slabs consisting of 60 atoms (12 unit cells, 6 atomic layers) exposing the SrO, BaO or TiO₂ terminated (100) facets (2x2) have been extracted from the bulk structure (Fig. S16). The slabs are surmounted by a 35 Å-thick layer of vacuum to ensure the energy convergence. During optimizations, only the 3 upper atomic layers are allowed to relax while the 3 lower are fixed to simulate the bulk of the material. The Brillouin zone was sampled with a 3 x 3 x 1 k-point grid. Electron occupancies were determined according to a gaussian scheme with an energy smearing of 0.1 eV.

CO₂ was adsorbed on the relaxed surfaces, and all adsorption parameters refer to the following adsorption reaction



The surface coverage obtained with one CO₂ molecule per unit cell is of 1.5 CO₂.nm⁻².

On the optimized systems, chemical shifts calculations were performed using the linear response method implemented in VASP. For these calculations, the convergence criterion on the SCF cycles was set to 10⁻⁸ eV. The reported chemical shifts are referenced to the gas-phase CO₂ for which $\delta(^{13}\text{C}) = 125.0$ ppm.

Thermodynamic calculations including enthalpic and entropic corrections were performed to calculate the Gibbs free energies by calculating the vibration frequencies for the gas-phase molecules and adsorbed species.⁶ The vibrational partition function is calculated from the calculated frequencies, and the molar vibrational enthalpy and entropy are derived. For the gas-phase CO₂, the additional contributions from the translation and rotation partition functions are considered, while they are considered equal to zero for the adsorbed species.

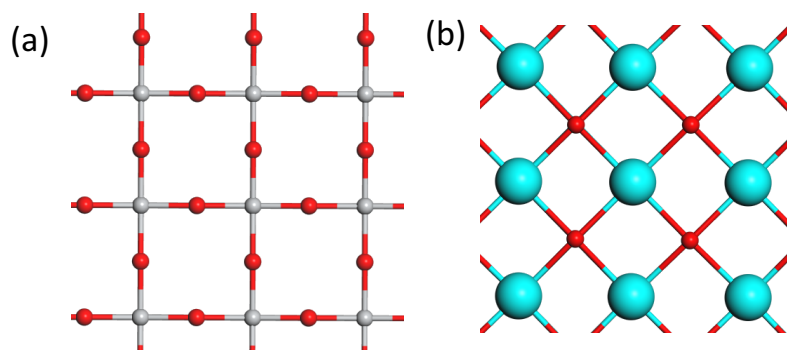


Fig. S19. Top view of the surface models for (a) the TiO_2 termination ($\text{SrTiO}_3\text{-TiO}_2$) (b) the SrO termination of SrTiO_3 ($\text{SrTiO}_3\text{-SrO}$). For BaTiO_3 , the structure is the same although with slightly different parameters, and referred to as $\text{BaTiO}_3\text{-TiO}_2$ and $\text{BaTiO}_3\text{-BaO}$. Red: O, Grey: Ti, Cyan: Sr, Green: Ba.

CO_2 adsorption on SrTiO_3

Table S4. Optimized structures of the adsorption modes of CO_2 on SrTiO_3 . Several geometric parameters are reported (distances in Å and angles in degrees). Red: O, Grey: Ti, Cyan: Sr.

Facet	Structure		$d_{\text{M-O}}$	$d_{\text{C-Os}}$	OCO angle
TiO_2 terminated	Carbonate		2.10	1.37	131
	Linear-vert.		2.49	-	180
SrO terminated	Carbonate		2.53	1.34	123
	Linear-vert.		2.82	-	180
	Linear-horiz.		2.87	-	176

Table S5. Adsorption enthalpies ($\text{kJ}\cdot\text{mol}^{-1}$) and entropies ($\text{J}\cdot\text{K}^{-1}\cdot\text{mol}^{-1}$) calculated at 298 K for the adsorption modes of CO_2 on SrTiO_3 . The calculated NMR parameters are also reported.

Facet	Structure	Energetics		^{13}C NMR parameters		
		$\Delta_{\text{ads}}H$ (298K)	$\Delta_{\text{ads}}S$ (298K)	δ_{iso} (ppm)	Ω (ppm)	κ
TiO_2 terminated	Carbonate	-128	-180	174	109	-0.83
	Linear-vert.	-13	-128	134	315	0.98
SrO terminated	Carbonate	-181	-174	180	97	-0.28
	Linear-vert.	-14	-102	132	350	0.99
	Linear-horiz.	-34	-135	140	373	0.85
$\text{CO}_{2(\text{g})}$		-	-	135	361	1.00

CO_2 adsorption on BaTiO_3

Table S6. Optimized structures of the adsorption modes of CO_2 on BaTiO_3 . Several geometric parameters are reported (distances in \AA and angles in degrees). Red: O, Grey: Ti, Green: Ba.

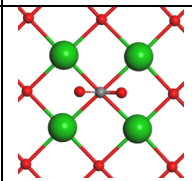
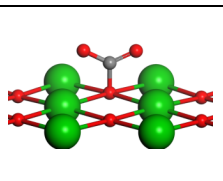
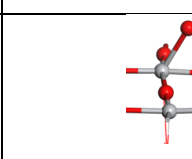
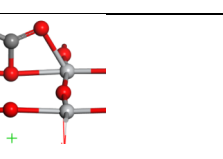
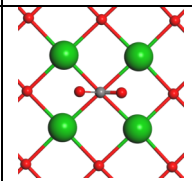
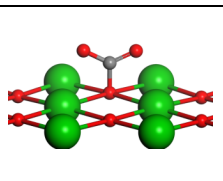
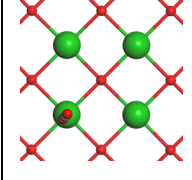
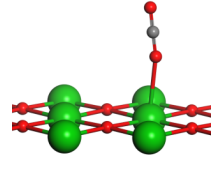
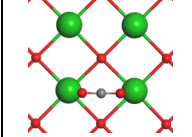
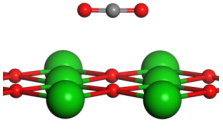
Facet	Structure			$d_{\text{M-O}}$	$d_{\text{C-Os}}$	OCO angle
TiO_2 terminated	Carbonate			2.10	1.35	131
	Linear-vert.			2.44	-	180
BaO terminated	Carbonate			2.95	1.37	129
	Linear-vert.			3.13	-	180
	Linear-horiz.			3.25	-	179

Table S7. Optimized structures of the adsorption modes of CO₂ on BaTiO₃. Several geometric parameters are reported (distances in Å and angles in degrees).

TiO ₂ terminated	Carbonate	-158	-183	174	104	-0.68
	Linear-vert.	-22	-116	131	343	0.99
BaO terminated	Carbonate	-165	-164	174	99	-0.89
	Linear-vert.	-7	-121	133	354	0.99
	Linear-horiz.	-22	-116	133	351	0.99
CO _{2(g)}		-	-	135	361	1.00

Comment on the adsorption energies

Experimental results clearly show that the adsorption of CO₂ on the surface of BaTiO₃ is stronger than on SrTiO₃. The calculated adsorption enthalpies on the TiO₂ terminated facets of both oxides are indeed in line with this, with stronger adsorption on TiO₂-BaTiO₃ than on TiO₂-SrTiO₃ ($\Delta_{\text{ads}}H^{\circ} = -158$ vs. -128 kJ.mol⁻¹, respectively). However, carbonates on the SrO-terminated facets of SrTiO₃ are more stable than carbonates on BaO-BaTiO₃ (-181 vs. -164 kJ.mol⁻¹), which is in disagreement with the experimental observations. Furthermore, on SrTiO₃, the linear CO₂ has a quite low calculated adsorption enthalpy, and thus it is expected for this species to easily turn into the more favorable carbonate. However, the linear CO₂ is definitely observed on SrTiO₃ by NMR (see Figure 3).

The comparison with the experimental results lead to the conclusion that the calculated adsorption the carbonate adsorbed on SrO-SrTiO₃ may be overestimated. A number of reason may be proposed, including coverage effects, local reconstruction of the surface, local electric fields... Investigating on such effects goes beyond the scope of this contribution, and thus we only use the DFT calculations to propose structures and assignments to the observed signals in ¹³C NMR.

REFERENCES

- (1) Kresse, G.; Furthmuller, J. *Phys. Rev. B* **1996**, *54*, 11169.
- (2) Kresse, G.; Hafner, J. *Phys. Rev. B* **1994**, *49*, 14251.
- (3) Perdew, J. P.; Burke, K.; Ernzerhof, M. *Phys. Rev. Lett.* **1996**, *77*, 3865.
- (4) Kresse, G.; Joubert, D. *Phys. Rev. B* **1999**, *59*, 1758.
- (5) Grimme, S.; Antony, J.; Ehrlich, S.; Krieg, H. *J. Chem. Phys.* **2010**, *132*.
- (6) Larmier, K.; Chizallet, C.; Cadran, N.; Maury, S.; Abboud, J.; Lamic-Humblot, A. F.; Marceau, E.; Lauron-Pernot, H. *ACS Cat.* **2015**, *5*, 4423.